Magn Reson Med Sci 2025; 24; 112–121
doi:10.2463/mrms.mp.2023-0127
Published Online: February 7, 2024

MAJOR PAPER

Peritumoral Fat Content Identified Using Iterative Decomposition of Water and Fat with Echo Asymmetry and Least-squares Estimation (IDEAL) Correlates with Breast Cancer Prognosis

Natsumi Hirano Tani[1], Yuki Koreeda[2], Aya Nawata[3], Akitaka Fujisaki[1], Yoshiko Hayashida[1], Shohei Shimajiri[4], Toshiyuki Nakayama[4], Masanori Hisaoka[3], Yuzuru Inoue[2], Keiji Hirata[2], Yuko Tashima[5], Fumihiro Tanaka[5], and Takatoshi Aoki[1*]

Purpose: Adipocytes around aggressive breast cancer (BC) are less lipid different from naive adipocytes (cancer-associated adipocytes, CAAs), and peritumoral edema caused by the release of cytokines from CAAs can conduce to decrease the peritumoral fat proportion. The purpose of this study was to correlate peritumoral fat content identified by using iterative decomposition of water and fat with echo asymmetry and least-squares estimation (IDEAL) with lymph node metastasis (LNM) and recurrence-free survival (RFS) in BC patients and to compare with T2-weighted (T2WI) and diffusion-weighted images (DWI) analyses.

Methods: This retrospective study consisted of 85 patients who were diagnosed with invasive carcinoma of breast and underwent breast MRI, including IDEAL before surgery. The scan time of fat fraction (FF) map imaging using IDEAL was 33s. Four regions of interest (ROIs), which are 5 mm from the tumor edge, and one ROI in the mammary fat of the healthy side were set on the FF map. Then average peritumoral FF values (TFF), average FF values on the healthy side (HFF), and peritumoral fat ratio (PTFR, which is defined as TFF/HFF) were calculated. Tumor apparent diffusion coefficient (ADC) values were measured on ADC map obtained by DWI. Peritumoral edema was classified into three grades based on the degree of signal intensity around the tumor on T2WI (T2 edema).

Results: The results of stepwise logistic regression analysis for four variables (TFF, PTFR, T2 edema, and ADC value) indicated that TFF and T2 edema were significant factors of LNM ($P < 0.01$). RFS was significantly associated with TFF ($P = 0.016$), and 47 of 49 (95.9%) patients with TFF more than 85.5% were alive without recurrence.

Conclusion: Peritumoral fat content identified by using IDEAL is associated with LNM and RFS and may therefore be a useful prognostic biomarker for BC.

Keywords: *adipose tissue, breast neoplasms, magnetic resonance imaging, prognosis, recurrence-free survival*

Introduction

Routine medical imaging has the potential to serve as a noninvasive biomarker to predict the biological behavior of cancer. Breast MRI is an important technique for the detection and diagnosis of breast cancer (BC) and for the local staging.[1–4] Breast edema, defined as high signal intensity on T2-weighted image (T2WI), is strongly associated with

[1]Department of Radiology, School of Medicine, University of Occupational and Environmental Health, Kitakyushu, Fukuoka, Japan
[2]Department of Surgery 1, University of Occupational and Environmental Health, Kitakyushu, Fukuoka, Japan
[3]Department of Pathology and Oncology, University of Occupational and Environmental Health, Kitakyushu, Fukuoka, Japan
[4]Department of Pathology and Cell Biology, School of Medicine, University of Occupational and Environmental Health, Kitakyushu, Fukuoka, Japan
[5]Department of Surgery 2, University of Occupational and Environmental Health, Kitakyushu, Fukuoka, Japan

*Corresponding author: Department of Radiology, University of Occupational and Environmental Health, 1-1 Iseigaoka, Yahatanishi-ku, Kitakyushu 807-8555, Japan. Phone: +81-93-691-7264, Fax: +81-93-692-0249,
E-mail: a-taka@med.uoeh-u.ac.jp

This work is licensed under a Creative Commons Attribution-NonCommercial-NoDerivatives International License.
©2025 Japanese Society for Magnetic Resonance in Medicine

Received: September 26, 2023 | Accepted: December 1, 2023

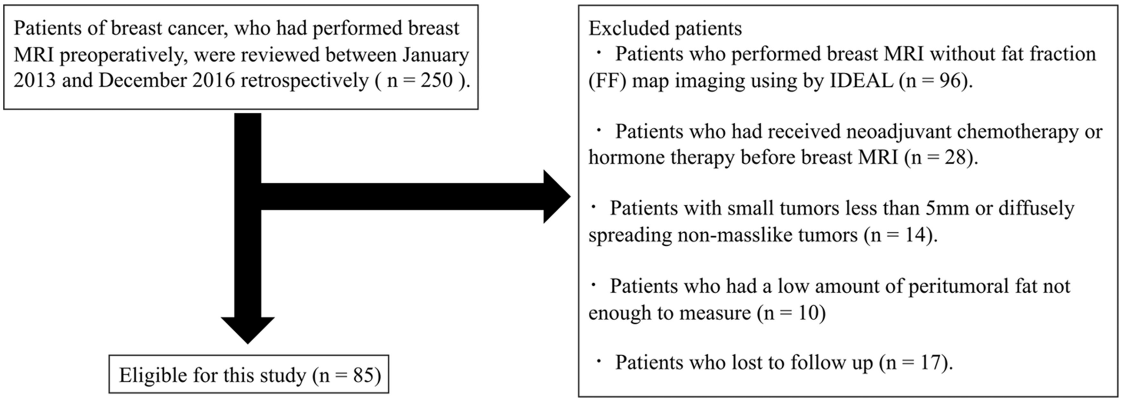

Fig. 1 Flow diagram for the patient selection process.

various prognostic factors in BC, such as lymphovascular invasion, lymph node metastasis (LNM), and histological grade, as previously reported in many studies.[5–7] In addition, the peritumoral edema identified at preoperative MR imaging can be used as an independent factor of disease recurrence.[8,9]

Lymph node status is one of the most important pathological prognostic factors in BC.[10] Several studies have been conducted on the relationship between apparent diffusion coefficient (ADC) values on preoperative diffusion-weighted images (DWI) and various biomarkers of BC, and some studies have reported that the ADC value of BC with LNM is lower than that without LNM.[11–13] However, according to some other research reports, ADC cannot predict LNM controversially.[14–16]

The infiltration of BC cells into adipocytes around tumors affects their proliferative and metastatic potential, local spread, and resistance to therapy.[17] *In vitro* and *in vivo* studies suggest that the surrounding adipocytes are modified by cancer cells to acquire characteristics different from those of naive adipocytes.[18] These adipocytes are called cancer-associated adipocytes (CAAs), secrete soluble factors (IL-6 and hepatocyte growth factor [HGF]), exosomes, and extracellular matrix components (matrix metalloproteinase-11 [MMP-11] and collagen IV), and then promote tumor cell invasiveness.[19,20] Histologically, CAAs around BC are smaller in size and have less lipid compared to naive adipocytes. Moreover, peritumoral edema due to cytokine release from CAAs may contribute to the reduced peritumoral fat proportion.[21]

Iterative decomposition of water and fat with echo asymmetry and least-squares estimation (IDEAL) is one of the recent MR techniques that can reliably separate fat and water using asymmetric echo times and the multipoint Dixon method.[22] Recently, IDEAL has been increasingly used in the studies of lipid metabolism in several organs.[23–25] Although there is only one prior study investigating the relationship between LNM and peritumoral fat content using IDEAL in BC patients,[26] a comparative study with other MR sequences has not been previously reported. In addition, no reports have documented the relationship between the peritumoral fat proportion obtained by IDEAL and the prognosis of BC patients.

The objective of this study was to correlate peritumoral fat content quantified by using IDEAL with LNM and recurrence-free survival (RFS) in BC patients and to compare with conventional MRI sequences, including T2WI and DWI.

Materials and Methods

Our hospital's institutional review board approved this study, and informed consent was waived.

Patients

Two-hundred and fifty BC patients, who had performed breast MRI preoperatively, were reviewed between January 2013 and December 2016 retrospectively. We excluded patients who performed breast MRI without fat fraction (FF) map imaging using IDEAL ($n = 96$), patients who had received neoadjuvant chemotherapy or hormone therapy before breast MRI ($n = 28$), patients with small tumors less than 5 mm or diffusely spreading non-masslike tumors ($n = 14$), and patients who had a low amount of peritumoral fat not enough to measure ($n = 10$). In addition, 17 lost to follow-up cases were excluded from the study. (Fig. 1). Clinical data, including age at BC diagnosis, date of MRI, date of surgery, tumor size, recurrence status, and survival, were obtained from medical records. Additional prognostic investigations were also performed as needed. RFS was defined as the time from the initial diagnosis to the diagnosis of BC recurrence.

Breast MRI protocol

Breast MRI was performed on a 3.0T unit (Discovery MR750w; GE Healthcare, Waukesha, WI, USA) using an eight-channel breast coil. All patients underwent breast MRI, covering the bilateral breasts in the prone position. The

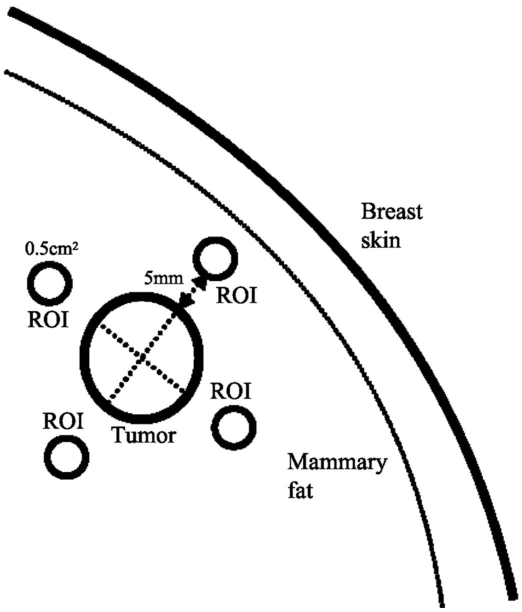

Fig. 2 Scheme illustrates peritumoral ROIs. In this study, four ROIs of 0.5 cm^2 on each crosshair were set 5 mm from the tumor, and all ROIs were placed within the mammary fat. ROIs, regions of interest.

patients had bilateral breast MRI, which included axial fat-suppression T2WI (TR: 4400 ms, TE: 91 ms, slice thickness: 5 mm, matrix: 416 × 384, and FOV: 33 × 33 cm), axial DWI (TR: 6000 ms, TE: 77 ms, slice thickness: 6 mm, matrix: 140 × 240, FOV; 36 × 36 cm, and *b* values: 0, 1500 s/mm^2), axial gadolinium-enhanced dynamic imaging, and axial IDEAL images. All the patients underwent IDEAL imaging before gadolinium-enhanced imaging. The IDEAL sequence was acquired with the following parameters: TR = 6.9 ms, 6 echoes/TR, TE min: 0.9 ms, TE spacing: 0.9–5.4 ms, slice thickness: 8 mm, FOV: 44 × 44 cm, matrix: 256 × 256, scan time: 33s.

Image assessment

Four regions of interest (ROIs) were manually set around BC on FF maps acquired by IDEAL. Each ROI was placed by one certificated radiologist, and the size of the ROI was 0.5 cm^2. The four ROIs in the mammary fat around the tumor were placed on each crosshair radial centered on the tumor, and each ROI was placed 5 mm away from the tumor margin (Fig. 2).[27] If the location of the ROI was placed in fibroglandular breast tissue, pectoralis major muscle, and outside the skin, it was manually moved to the adjacent breast fat. In the patients with multiple lesions, the ROIs were set for the largest lesion. When setting ROIs at the four locations, ROIs were set in a direction that did not overlap the nonadipose tissue as much as possible. In addition, we also set one ROI at arbitrarily location within the mammary fat of the healthy side on the FF map. DWI and post-contrast T1WI were referenced to set the ROIs. The obtained values were then applied to the respective formulae to obtain the mean FF value around the tumor (TFF), the mean FF value on the healthy side (HFF), and the peritumoral fat ratio (PTFR, which is defined as TFF/HFF). HFF was only used for PTFR calculation.

Moreover, we placed a circular ROI in the darkest part of the tumor on the ADC map generated by DWI. The ROI sizes varied due to the darkest part sizes. To avoid mistakenly measuring low ADC values unrelated to the tumor, the ROI was sized to fit within the enhanced area of the lesion and placed to avoid artifacts, necrotic and bleeding areas of the lesion, and non-enhancing lesions while referring to other MR images.

Peritumoral edema on T2WI (T2 edema) was classified into three grades (0–2) based on the degree of signal intensity around the tumor according to the previously described grading method[8] as follows (Fig. 3): Grade 0 indicates a lack of high signal intensity around the BC; Grade 1 indicates moderately high signal intensity around the BC but is lower than that of water; and Grade 2 indicates signal intensity around the BC similar to that of water.[8] The highest signal around the BC was evaluated. All the image assessments were blinded to histopathologic information, LNM, and prognosis.

Histological analysis

The histological data were determined based on surgically excised tissues and lymph node biopsy tissues. The histopathological specimens used in this study were all reviewed by two certified pathologists blinded to all the MRI findings, and the final decision was made by their consensus. They also retrospectively evaluated the histopathological features (fibrous/edematous, atrophy of fat cells, inflammatory cells proliferation, etc.) surrounding BC (area 5 mm from tumor edge) between BC patients with LNM and those without blinded to the prognosis.

Statistical analysis

In this study, we investigated whether there were differences in each of the four variables (TFF, PTFR, T2 edema, and ADC value) obtained by each sequence of MRI between BC patients with and without LNM using a non-parametric Mann–Whitney U test. Multiple regression analysis was performed by a forward stepwise logistic regression model using these four variables. Receiver operating characteristics (ROC) and area under the curve (AUC) calculations were performed to evaluate the diagnostic performance of the best model. The optimal cutoff value for predicting recurrence or metastasis in the ROC curve was determined by the maximum value (sensitivities + specificities) of Youden index. Patients were classified into high TFF and low TFF groups according to this value. Moreover, RFS according to each variable was also compared using Kaplan–Meier analysis and Cox proportional hazards regression. We performed all statistical calculations using

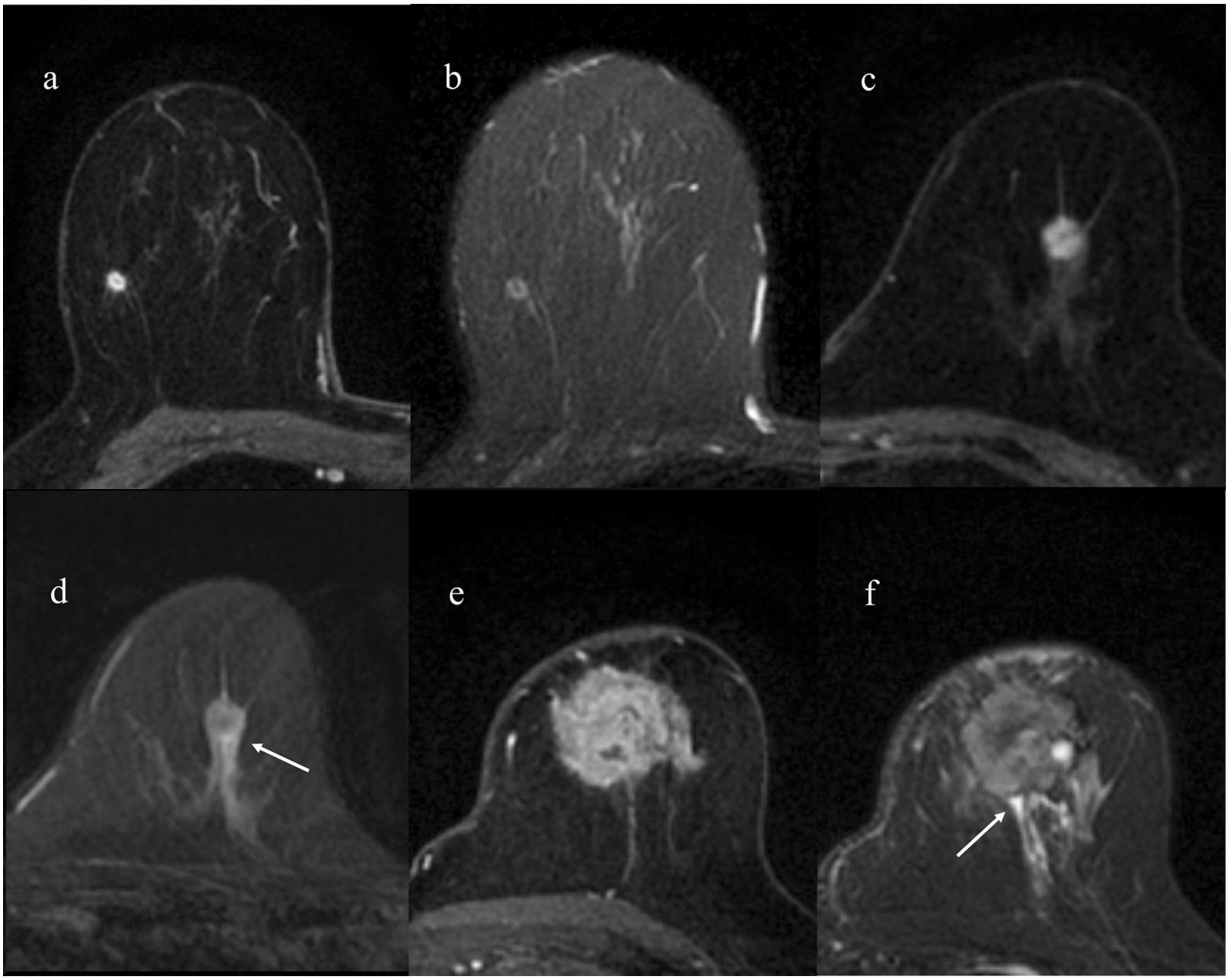

Fig. 3 Peritumoral edema surrounding the tumor on T2-weighted MR images. (**a** and **b**) Grade 0: axial fat-suppressed post-contrast T1-weighted (**a**) and T2-weighted (**b**) images indicate an absence of high signal intensity. (**c** and **d**) Grade 1: axial fat-suppressed post-contrast T1-weighted (**c**) and T2-weighted (**d**) images indicate that the signal intensity surrounding the tumor is moderately high but is less than that of water (arrow in **d**). (**e** and **f**) Grade 2: axial fat-suppressed post-contrast T1-weighted (**e**) and T2-weighted (**f**) images indicate that the signal intensity surrounding the tumor is as high as that of water (arrow in **f**).

IBM SPSS Statistics, version 22.0 (IBM, Armonk, NY, USA). The significance level was set at $P < 0.05$ in all statistical tests.

Results

Finally, 85 patients (age range 36–83 years and median 62.8 years) with 85 lesions were included in this study. Tumor sizes ranged from 5 to 56 mm (mean, 20.1 mm). The patient characteristics of the 85 patients are summarized in Table 1. The median follow-up period for the RFS was 2392 days (range, 41–3068 days).

Table 2 shows comparisons of four MRI-derived variables between the LNM and non-LNM groups. There were significant differences in TFF ($P < 0.001$), PTFR ($P = 0.002$), and T2 edema ($P = 0.004$) between the two groups. The TFF and the PTFR between BC with LNM were significantly lower than those without LNM. On the other hand, the ADC value was not significantly different between the two groups ($P = 0.6$). Multivariate logistic regression showed that TFF and T2 edema were independently associated factors for LNM ($P < 0.05$) (Table 3). Moreover, the diagnostic performance to predict LNM by the best model combined TFF and T2 edema was evaluated using ROC curves, and AUC of the best model was 0.836.

The ROC analysis for LNM status was used to identify the optimal cutoff point of TFF (value = 85.5, achieving the Youden index), and patients were divided into low

Table 1 Patient characteristics of the 85 breast carcinoma patients

ER	Positive	60
	Negative	25
PgR	Positive	52
	Negative	33
HER2	Positive	18
	Negative	67
Tumor subtype	Triple negative – a spectrum of ER/HER2 negative	14
	Hormone receptor negative and HER2 positive	11
	Hormone receptor positive and HER2 positive	21
	Hormone receptor positive and HER2 negative	0
	High receptor, low proliferation, and low grade (luminal A-like)	34
	Low receptor, high proliferation, and high grade (luminal B-like)	5

ER, estrogen receptor; HER2, human epidermal growth factor receptor type 2; PgR, Progesterone receptor.

Table 2 Comparison of four variables (TFF, PTFR, T2 edema, and ADC value) between breast carcinoma with LNM and that without LNM

Factors	LNM		*P* value
	Positive	Negative	
TFF	78.56 ± 10.47	86.51 ± 4.44	<0.001
PTFR	0.89 ± 0.08	0.95 ± 0.03	0.002
T2 edema	1.35 ± 0.93	0.65 ± 0.81	0.004
ADC value ($\times 10^{-3}$ mm^2/s)	0.92 ± 0.14	0.90 ± 0.22	0.6

ADC, apparent diffusion coefficient; LNM, lymph node metastasis; PTFR, peritumoral fat ratio; TFF, tumor fat fraction.

Table 3 Multivariate logistic regression analysis of factors associated with lymph node metastasis for four variables (TFF, PTFR, T2 edema, and ADC value)

Factors	Standardized regression coefficient	*P* value
TFF	−.442	<0.0001
T2 edema	.234	0.017

ADC, apparent diffusion coefficient; PTFR, peritumoral fat ratio; TFF, tumor fat fraction. PTFR and ADC value were unselected predictors.

TFF (≤85.5) and high TFF groups (>85.5). There was a significant difference in RFS between the two groups (P = 0.016), and the low TFF group had poorer prognoses than the high TFF group (hazard ratio 5.4; 95% CI, 1.15–25.62) (Fig. 4). Forty-seven of 49 (95.9%) patients with TFF more than 85.5% were alive without recurrence. Although there was a trend toward poorer prognoses in the Grade 2 group compared to the Grade 0 and 1 groups, no statistically significant difference in RFS was identified (P = 0.076) among the three groups according to T2 edema grade (Fig. 5).

Figures 6 and 7 show representative cases of BC patients with postoperative recurrence. In both cases, fat-suppressed T2WI showed a hyperintense mass in the breast, and the corresponding TFF around the tumor on the FF map using IDEAL was low. Peritumoral edema on fat-suppressed T2WI is found in one case (Fig. 7) but not in another (Fig. 6).

Histologically, the peritumoral fatty tissue of BCs with poor prognosis was noticeably fibrotic and edematous compared to those without LNM and/or recurrence. In addition, atrophy of fat cells and mild inflammatory cell infiltration were more frequently observed in the adipose tissue around BC with poor prognosis (Fig. 8). In addition, the MRI images corresponding to these cases are illustrated in Fig. 9.

Discussion

The results of this study revealed that peritumoral fat content using IDEAL is significantly associated with LNM and RFS. On multiple regression analysis using four variables (TFF, PTFR, T2 edema, and ADC value) derived from breast MRI, TFF was one of the significant factors of LNM (P < 0.01), and the model that included TFF and T2 edema showed high diagnostic performance (AUC = 0.836) for LNM status. Furthermore, 47 of 49 (95.9%) BC patients with high TFF values were alive without recurrence. Quantification of the peritumoral fat content using IDEAL may predict the prognosis of BC patients *in vivo*.

Although a statistically significant difference in RFS was not identified among the three groups according to T2 edema, there was a significant difference in RFS between the high and the low TFF groups. In addition, our results demonstrated that TFF was an independent predictive factor of LNM as well as T2 edema. Histologically, peritumoral adipose tissue of the BCs with poor prognosis was revealed to be more fibrous and edematous and tended to be less lipid with inflammatory cells compared with that without recurrence. Quantification of peritumoral fat proportion is thought to be caused not only by peritumoral edema due to the release of cytokines[21,28,29] but also by various factors such as fibrosis, atrophy of fat cells, and cell infiltration, such as lymphocytes, bone-marrow-derived inflammatory cells, and fibroblasts.[30,31] The nonmalignant cells in the tumor microenvironment often play a pro-tumorigenic function at all phases of carcinogenesis by stimulating uncontrolled cell proliferation. A decrease in the peritumoral

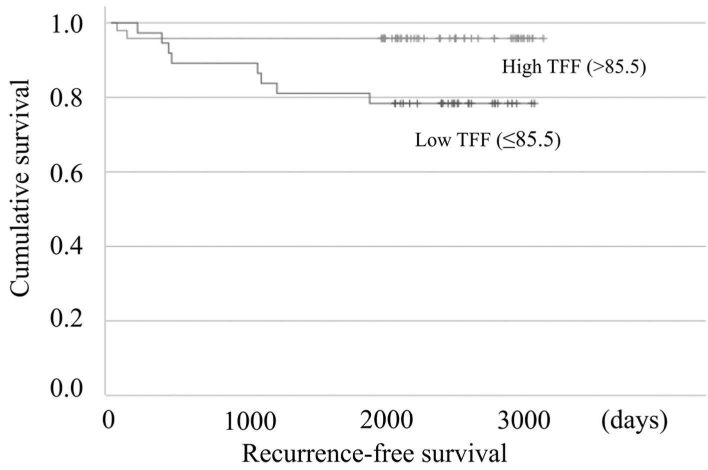

Fig. 4 Recurrence-free survival according to TFF using IDEAL. Recurrence-free survival was associated with TFF ($P = 0.016$). TFF, tumor fat fraction.

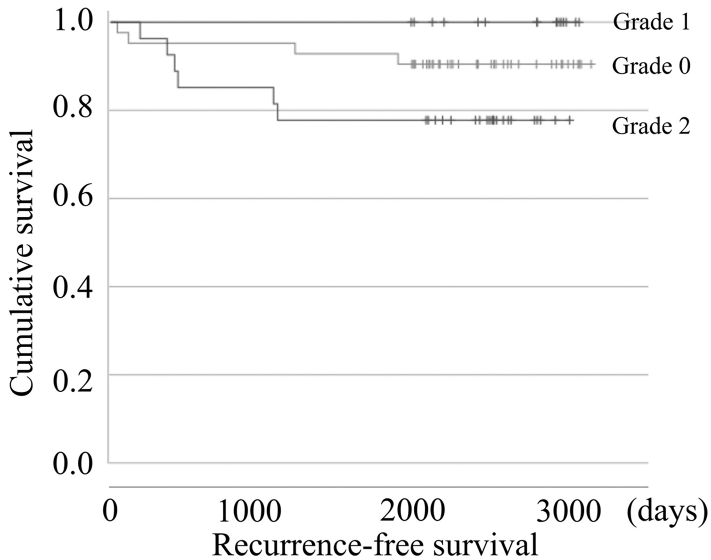

Fig. 5 Recurrence-free survival according to T2 edema. Recurrence-free survival was not significantly associated with T2 edema ($P = 0.076$).

fat content on IDEAL can potentially provide additional information to T2 edema for the prediction of BC patients' prognosis.

IDEAL is less affected by both the heterogeneity of the main magnetic field (B0) and the high-frequency magnetic field (B1) and excels in the homogeneity of fat suppression.[22,32,33] Therefore, it is less susceptible to magnetic field inhomogeneity due to the shape of the breast, making it possible to stably quantify the amount of fat. IDEAL is simple to perform in a short time (33s) without an extrinsic contrast agent. IDEAL imaging adding to the conventional MRI is unlikely to be a burden on the patient with BC. Fat quantification using the IDEAL could be an easy-to-implement clinical tool for treatment strategies of BC patients.

There were several limitations in this study. First, in order to examine the influence of peritumoral tissue, diffuse non-mass-like lesions were not included in this study. Additional study is necessary for evaluating the clinical implications of the peritumoral fat quantification in these types of tumors. Second, the ROI was manually set to visually decide the fat area, avoiding fibroglandular breast tissue, by one radiologist. The use of computed automatic ROI setting software may overcome subjective problems and improve reproducibility. Third, the cases in which there was a low amount of

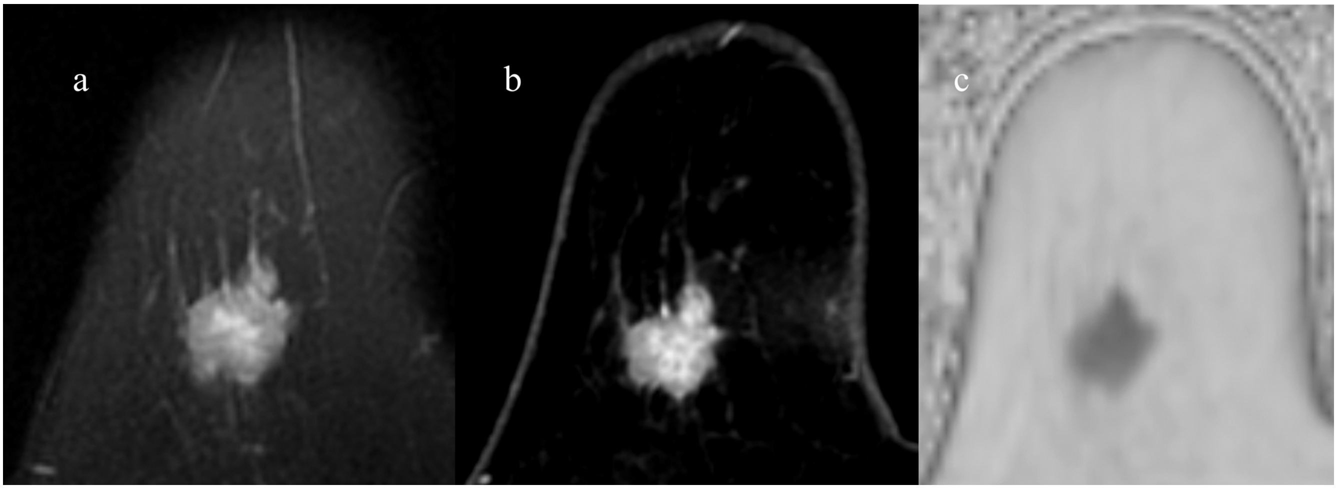

Fig. 6 Preoperative right breast MR images in a 62-year-old woman with a 20-mm invasive ductal carcinoma (luminal A type). Axial fat-suppressed post-contrast T1-weighted image (**a**) shows a 20-mm high-intensity mass in the right breast. The fat-suppressed T2-weighted image (**b**) shows the high-intensity mass without edema in the right breast, and the corresponding average peritumoral TFF (85.15) on the fat fraction map (**c**) is low. A local recurrence appeared 4 years and 11 months after surgery. TFF, tumor fat fraction.

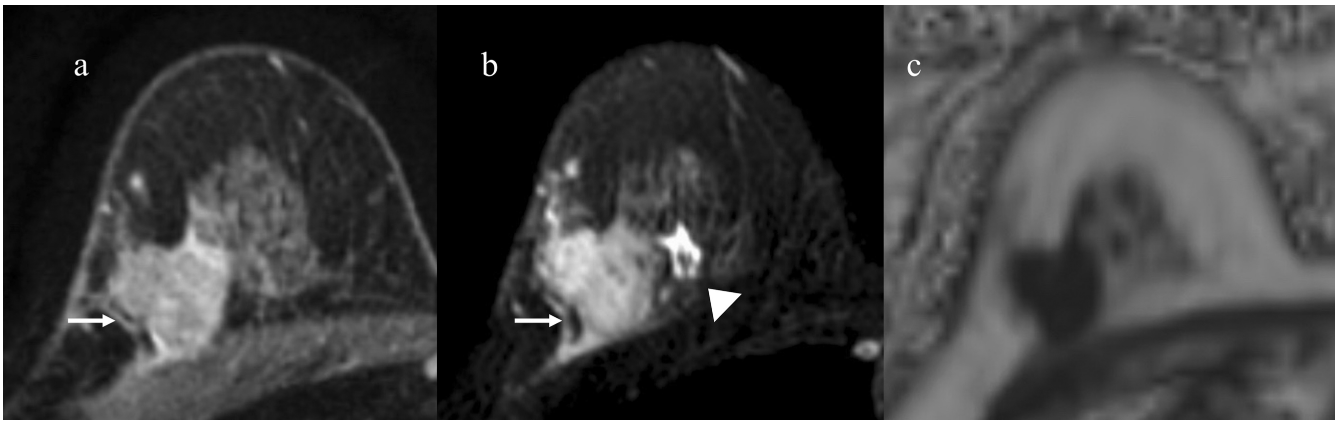

Fig. 7 Preoperative right breast MR images in a 64-year-old woman with a 29-mm invasive ductal carcinoma (triple negative type). Axial fat-suppressed post-contrast T1-weighted image (**a**) shows a 29-mm high-intensity mass (arrow) in the right breast. The fat-suppressed T2-weighted image (**b**) shows the high-intensity mass (arrow) with Grade 2 edema (arrowhead) in the right breast, and the corresponding average peritumoral TFF (80.16) on the fat fraction map (**c**) is low. A local recurrence appeared 1 year and 10 months after surgery. TFF, tumor fat fraction.

peritumoral fat, not enough to measure, were excluded from the study. This quantification method may not be applicable to dense breasts. Fourth, we cannot rule out the possibility that the difference in surgical management and the chemotherapy among the BC patient groups have had an impact on RFS. Finally, this study included a relatively small number of patients at a single site. Further multicenter prospective studies with a greater number of cases are likely necessary to confirm the clinical usefulness of peritumoral fat content quantification using IDEAL.

Conclusion

Our study indicates that the peritumoral fat content using IDEAL appears to be closely related to LNM and RFS. *In vivo* IDEAL imaging is simple to perform, and the quantification of the peritumoral fat content identified by using IDEAL may be useful for therapeutic strategies for BC patients.

Conflicts of Interest

The authors declare that they have no conflicts of interest.

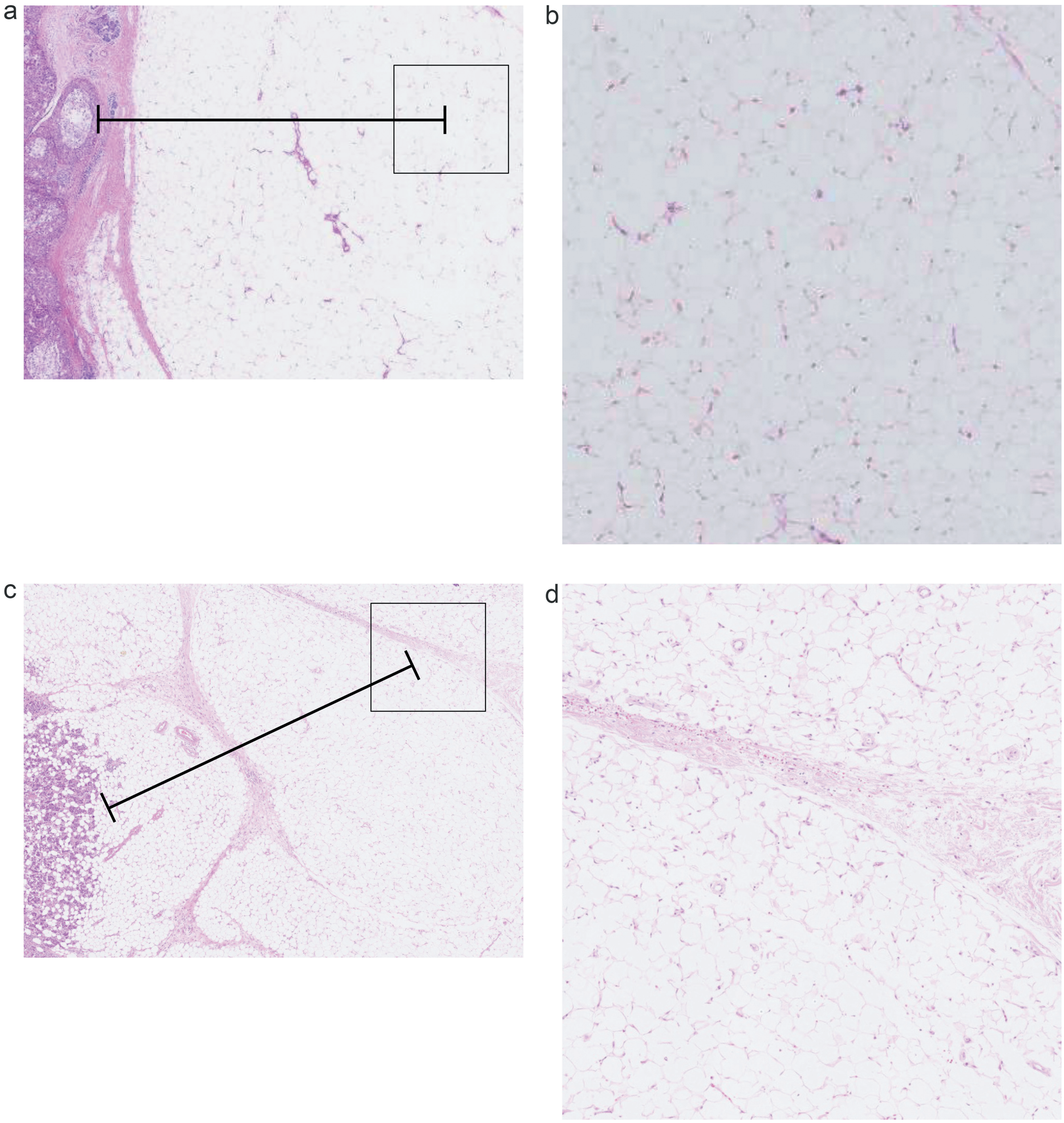

Fig. 8 Pathological findings (hematoxylin-eosin stain) of the peritumoral area of the breast carcinoma (**a** and **c**: low-power view, **b** and **d**: magnified view). Peritumoral adipose tissue of breast carcinoma with LNM (**c** and **d**) revealed to be more fibrous and edematous compared to that without LNM (**a** and **b**). In addition, mild inflammatory cell infiltration and atrophy of adipocyte tended to be more common in the peritumoral adipose tissue of breast carcinoma with LNM (**c** and **d**). The patient had lung and skin metastases 6 months after surgery. LNM, lymph node metastasis.

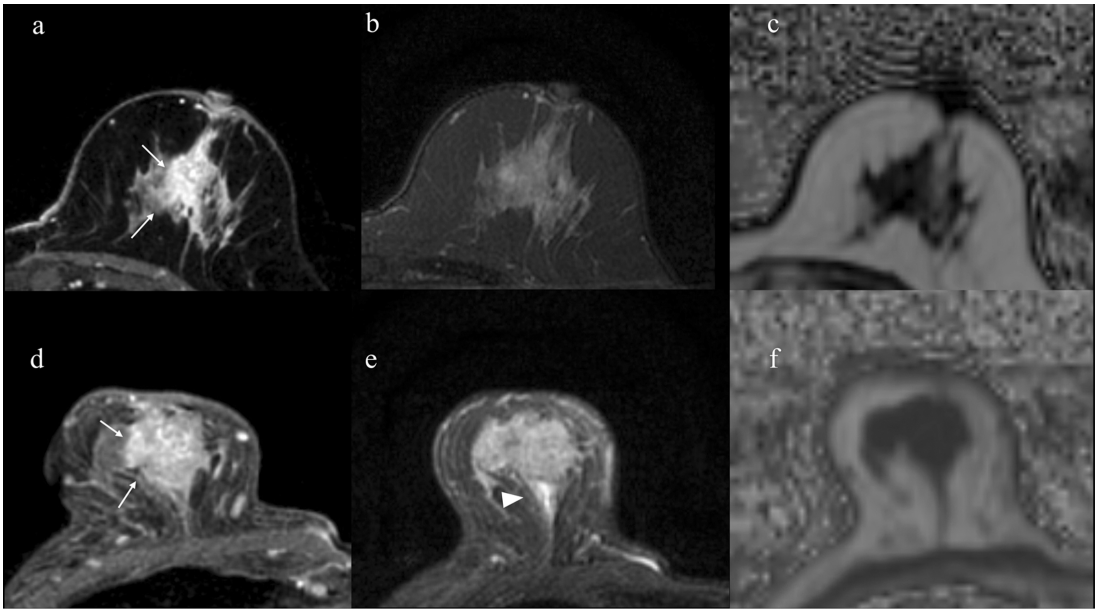

Fig. 9 MR images of the cases shown in Fig. 8. (**a**–**c**: case without recurrence and LNM, **d** and **f**: case with recurrence and LNM). In the case with good prognosis, a high-intensity mass (arrow) in the left breast on axial fat-suppressed post-contrast T1-weighted image (**a**) and no edema on fat-suppressed T2-weighted image (**b**) are shown, and the corresponding average peritumoral TFF (91.075) on the fat fraction map (**c**) is high. In the case with poor prognosis, a high-intensity mass (arrow) in the left breast on axial fat-suppressed post-contrast T1-weighted image (**d**) and the high signal intensity surrounding the tumor (arrowhead) on fat-suppressed T2-weighted image (**e**) are shown, and the corresponding average peritumoral TFF (67.875) on the fat fraction map (**f**) is low. LNM, lymph node metastasis; TFF, tumor fat fraction.

References

1. Orel SG, Schnall MD. MR imaging of the breast for the detection, diagnosis, and staging of breast cancer. *Radiology* 2001; 220:13–30.
2. Kuhl C. The current status of breast MR imaging. Part 1. Choice of technique, image interpretation, diagnostic accuracy, and transfer to clinical practice. *Radiology* 2007; 244:356–378.
3. Mann RM, Cho N, Moy L. Breast MRI: State of the art. *Radiology* 2019; 292:520–536.
4. Park NJ, Jeong JY, Park JY, et al. Peritumoral edema in breast cancer at preoperative MRI: An interpretative study with histopathological review toward understanding tumor microenvironment. *Sci Rep* 2021; 11:12992.
5. Çetinkaya E, Yıldız Ş, Otçu H, Sharifov R, Yabul FÇ, Alkan A. The value of adjacent vessel sign in malignant breast tumors. *Diagn Interv Radiol* 2022; 28:463–469.
6. Xu Z, Ding Y, Zhao K, et al. MRI characteristics of breast edema for assessing axillary lymph node burden in early-stage breast cancer: A retrospective bicentric study. *Eur Radiol* 2022; 32:8213–8225.
7. Lee HJ, Lee JE, Jeong WG, et al. HER2-positive breast cancer: Association of MRI and clinicopathologic features with tumor-infiltrating lymphocytes. *AJR Am J Roentgenol* 2022; 218:258–269.
8. Cheon H, Kim HJ, Kim TH, et al. Invasive breast cancer: Prognostic value of peritumoral edema identified at preoperative MR Imaging. *Radiology* 2018; 287:68–75.
9. Uematsu T, Kasami M, Watanabe J. Is evaluation of the presence of prepectoral edema on T2-weighted with fat-suppression 3 T breast MRI a simple and readily available noninvasive technique for estimation of prognosis in patients with breast cancer?. *Breast Cancer* 2014; 21:684–692.
10. Fisher B, Bauer M, Wickerham DL, et al. Relation of number of positive axillary nodes to the prognosis of patients with primary breast cancer. An NSABP update. *Cancer* 1983; 52:1551–1557.
11. Belli P, Costantini M, Bufi E, et al. Diffusion magnetic resonance imaging in breast cancer characterisation: Correlations between the apparent diffusion coefficient and major prognostic factors. *Radiol Med (Torino)* 2015; 120:268–276.
12. Dorrius MD, Dijkstra H, Oudkerk M, Sijens PE. Effect of b value and pre-admission of contrast on diagnostic accuracy of 1.5-T breast DWI: A systematic review and metaanalysis. *Eur Radiol* 2016; 85:1651–1658.
13. Igarashi T, Furube H, Ashida H, Ojiri H. Breast MRI for prediction of lymphovascular invasion in breast cancer patients with clinically negative axillary lymph nodes. *Eur J Radiol* 2018; 107:111–118.
14. Kim SH, Cha ES, Kim HS, et al. Diffusion-weighted imaging of breast cancer: Correlation of the apparent diffusion coefficient value with prognostic factors. *J Magn Reson Imaging* 2009; 30:615–620.
15. Choi SY, Chang YW, Park HJ, Kim HJ, Hong SS, Seo DY. Correlation of the apparent diffusion coefficiency values on diffusion-weighted imaging with prognostic factors for breast cancer. *Br J Radiol* 2012; 85:e474–e479.
16. Surov A, Chang YW, Li L, et al. Apparent diffusion coefficient cannot predict molecular subtype and lymph node metastases

in invasive breast cancer: A multicenter analysis. *BMC Cancer* 2019; 19:1043.

17. Duong MN, Geneste A, Fallone F, Li X, Dumontet C, Muller C. The fat and the bad: Mature adipocytes, key actors in tumor progression and resistance. *Oncotarget* 2017; 8:57622–57641.
18. Nieman KM, Kenny HA, Penicka CV, et al. Adipocytes promote ovarian cancer metastasis and provide energy for rapid tumor growth. *Nat Med* 2011; 17:1498–1503.
19. Dirat BA, Bochet L, Escourrou G, Valet P, Muller C. Unraveling the obesity and breast cancer links: A role for cancer-associated adipocytes?. *Endocr Dev* 2010; 19:45–52.
20. Wu Q, Li B, Li Z, Li J, Sun S, Sun S. Cancer-associated adipocytes: Key players in breast cancer progression. *J Hematol Oncol* 2019; 12:95.
21. Dirat B, Bochet L, Dabek M, et al. Cancer-associated adipocytes exhibit an activated phenotype and contribute to breast cancer invasion. *Cancer Res* 2011; 71:2455–2465.
22. Reeder SB, Wen Z, Yu H, et al. Multicoil Dixon chemical species separation with an iterative least squares estimation method. *Magn Reson Med* 2004; 51:35–45.
23. Ma J, Song Z, Yan F. Detection of hepatic and pancreatic fat infiltration in type II diabetes mellitus patients with IDEAL-Quant using 3.0T MR: Comparison with single-voxel proton spectroscopy. Chin Med J (Engl) 2014; 127:3548–3552.
24. Guo RM, Li QL, Luo ZX, et al. In vivo assessment of neurodegeneration in Type C Niemann-Pick disease by IDEAL-IQ. *Korean J Radiol* 2018; 19:93–100.
25. Ma Q, Cheng X, Hou X, Yang Z, Ma D, Wang Z. Bone marrow fat measured by a chemical shift-encoded sequence (IDEAL-IQ) in patients with and without metabolic syndrome. *J Magn Reson Imaging* 2021; 54:146–153.
26. Hisanaga S, Aoki T, Shimajiri S, et al. Peritumoral fat content correlates with histological prognostic factors in breast carcinoma: A study using iterative decomposition of water and fat with echo asymmetry and least-squares estimation (IDEAL). *Magn Reson Med Sci* 2021; 20:28–33.
27. Lu S, Ahn D, Johnson G, Cha S. Peritumoral diffusion tensor imaging of high-grade gliomas and metastatic brain tumors. AJNR Am J Neuroradiol 2003; 24:937–941.
28. Baltzer PA, Yang F, Dietzel M, et al. Sensitivity and specificity of unilateral edema on T2w-TSE sequences in MR-Mammography considering 974 histologically verified lesions. *Breast J* 2010; 16:233–239.
29. Smolanka II, Bagmut IY, Movchan OV, et al. Features of VEGF and IL-6 expression in patients with inflammatory breast cancer considering molecular-biological characteristics. *J Med Life* 2023; 16:153–159.
30. Arneth B. Tumor microenvironment. *Medicina (Kaunas)* 2020; 56:15.
31. Spill F, Reynolds DS, Kamm RD, Zaman MH. Impact of the physical microenvironment on tumor progression and metastasis. *Curr Opin Biotechnol* 2016; 40:41–48.
32. Aoki T, Yamaguchi S, Kinoshita S, Hayashida Y, Korogi Y. Quantification of bone marrow fat content using iterative decomposition of water and fat with echo asymmetry and least-squares estimation (IDEAL): Reproducibility, site variation and correlation with age and menopause. *Br J Radiol* 2016; 89:20150538.
33. Gerdes CM, Kijowski R, Reeder SB. IDEAL imaging of the musculoskeletal system: Robust water fat separation for uniform fat suppression, marrow evaluation, and cartilage imaging. *AJR Am J Roentgenol* 2007; 189:W284–91.